

Magnetic Circular Dichroism in $3d-2p$ X-Ray Emission

Pieter KUIPER*

Department of Physics, Uppsala University, Box 530, S-751 21 Uppsala, Sweden

(Received July 26, 1999)

Magnetic circular dichroism in XAS, XPS, and XES at the $2p$ levels of magnetic $3d$ transition metals is analyzed using a pedagogical method. A back-of-the-envelope analysis of the dichroism in X-ray absorption is extended to circular dichroism in $2p$ photoemission. X-ray emission from the polarized $2p$ core holes is then analyzed using the same graphic single-particle model. The fact that spin is not a constant of motion at the spin-orbit split $2p$ levels is included. This gives MCD ratios of L_β emission that are much smaller and in much better agreement with experiment than those predicted by [Jo and Parlebas: *J. Phys. Soc. Jpn.* **68** (1999) 1392]. The same analysis is also applied to dichroism in X-ray emission on the L_2 and L_3 absorption resonances.

KEYWORDS: magnetic circular dichroism, XPS, XES, spin-orbit coupling, $2p$ -core level

§1. Introduction

Since the first measurements of the strong magnetic circular dichroism (MCD) in X-ray absorption at the L -edges of nickel,¹⁾ dichroism effects involving the $2p$ levels of the important magnetic $3d$ transition metals have been widely studied. Dichroism was also detected in the $2p$ XPS spectrum.²⁾ A prediction of magnetic dichroism in X-ray emission³⁾ led to experiments by several groups,⁴⁻⁷⁾ but the predicted lineshapes have not been reliably observed, and even the magnitude of the dichroic effect is not explained.

Atomic calculations have been very successful in reproducing the size and the rich detailed structure of MCD spectra.⁸⁾ But a simple single-particle model has its uses. It was even able to predict the basic features of MCD.⁹⁾ This model has been put in a very pedagogical form with back-of-the-envelope histograms by Jo.¹⁰⁾ In this paper I will show how this graphic method can be extended to derive the shape of magnetic dichroism in $2p$ XPS. Dichroism in X-ray emission (the radiative decay of these core hole states) can also be deduced from the histograms. One needs to take into account that spin is not a good quantum number for the spin-orbit split $2p_{1/2}$ and $2p_{3/2}$ levels. In a recent paper giving a basic treatment of X-ray emission, Jo and Parlebas¹¹⁾ have neglected this and found unrealistically large MCD effects in L_β (continuum-excited $2p_{1/2}$) emission.

The purpose of this paper is not to obtain quantitative results. The model is not realistic: it does not include orbital moment, correlation, intermediate coupling, etcetera. My main purpose here is to elucidate the consequences of spin not being a constant of motion of transition metal $2p$ levels. Readers may also find the histogram drawings useful in keeping track of the sign of the dichroism effects.

§2. XAS and XPS

My presentation is based on Jo's diagrams.^{10,12)} Figure 1 shows the distribution of the spin-orbit coupled $2p$ states over the orbital and spin quantum numbers separately for the $2p_{3/2}$ levels, where the spin is parallel to the orbital moment, and for the $2p_{1/2}$ levels, where the spin is antiparallel to the orbital moment. In both diagrams the hatched area gives the weights of orbital and spin quantum numbers of the eigenstates with the azimuthal quantum number $m_j = 1/2$. The areas of the other m_j levels can easily be deduced. At the $j = 3/2$ level, the levels with $m_j = \pm 3/2$ are pure spin states. However, all $m_j = \pm 1/2$ levels are superpositions of opposite spin directions with weights one-third and two-thirds. It will be shown that this limits the strength of the emission dichroism at the $2p_{1/2}$ level.

Figure 2 shows the relative transition probabilities for circularly polarized light with positive helicity ($\Delta m = +1$), negative helicity ($\Delta m = -1$) and linearly polarized light parallel to the z direction ($\Delta m = 0$). The probabilities are given for d -wave photoelectrons with different final azimuthal quantum numbers m_d . With unpolarized light, the sum of these contributions gives all m_d -levels equal intensities. The numbers in Fig. 2 are proportional to the squares of Wigner $3j$ symbols.¹³⁾ In this case $j_1 = 2$ for the d photoelectron, $j_3 = 1$ for the core level, and $j_2 = 1$ for the photon. The polarization dependence is obtained by taking $m_2 = -1, 0, 1$. Just to give two examples for $p-d$ transitions with z -polarized light:

$$\begin{pmatrix} 2 & 1 & 1 \\ -1 & 0 & 1 \end{pmatrix} = -\sqrt{\frac{3}{30}} \quad \text{and} \quad \begin{pmatrix} 2 & 1 & 1 \\ 0 & 0 & 0 \end{pmatrix} = \sqrt{\frac{4}{30}}.$$

By multiplying the coefficients for positive helicity of Fig. 2 with the ground state distribution of Fig. 1 one arrives at the distribution of $2p$ hole states in Fig. 3. For excitation from the $2p_{3/2}$ -level the ratio of the spin-up area to the spin-down area is 5:3. At the $2p_{1/2}$ -level this ratio is 1:3. In order to obtain the dichroism in X-ray

* E-mail: Pieter.Kuiper@fysik.uu.se

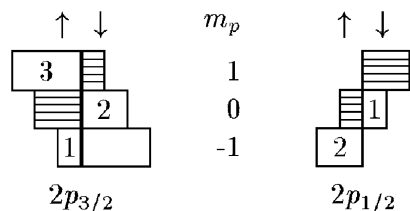


Fig. 1. The distribution of the weight of $2p$ orbital and spin quantum number over the $2p_{3/2}$ and $2p_{1/2}$ levels. The hatched areas represent the states with $m_j = 1/2$ states.

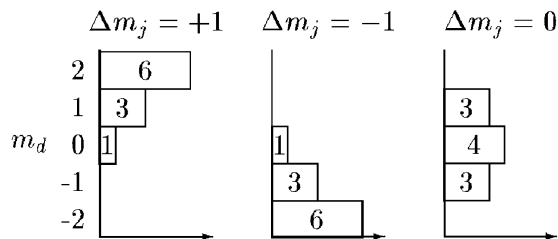


Fig. 2. The dependence on the $p \rightarrow d$ matrix element on the d azimuthal quantum number for positive, negative and zero helicity.

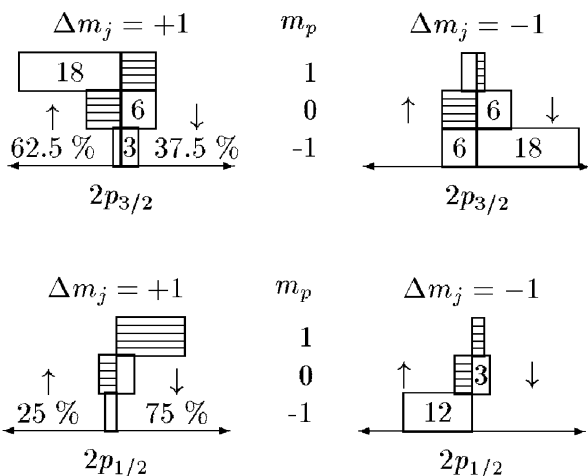


Fig. 3. The final state of $p \rightarrow d$ photoemission for light with positive and negative helicity. Percentages indicate the spin of the d wave photoelectron. The hatched areas give the weight of the p hole states with $m_j = 1/2$. The ratios of the weights are 18:12:7:3 for $j = 3/2$ and 15:5 for $j = 1/2$.

absorption, the $3d$ band may be regarded as a spin analyzer. If there are only unoccupied states for minority (\uparrow) $3d$ electrons, one arrives at an MCD ratio for positive to negative light of 5:3 for strong ferromagnets at the L_3 edge.¹⁰⁾ This is of the correct order of magnitude. Deviations are caused by the orbital moment of the $3d$ electrons or by the effect of strong $3d$ electrostatic interactions.¹²⁾

The shape of the circular dichroism in XPS can also be deduced from Fig. 3. By taking the total area of each m_j eigenstate, one can construct the histogram of Fig. 4. The intensity of the eigenstates is plotted in the order of their binding energies, given by the spin-orbit splitting and the exchange with the $3d$ spin moment. For photoe-

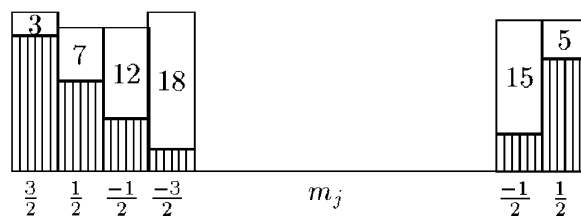


Fig. 4. Photoemission intensities for excitation of $2p$ electrons to d -wave electrons, for light with positive helicity (hatched) and negative helicity (numbers).

mission by X-ray with positive helicity, the $m_j = 1/2$ intensity at the $2p_{1/2}$ -level is three times as large as that of the state with $m_j = -1/2$. For light with negative helicity, this ratio is the other way around. At the $2p_{3/2}$ -level the four m_j states have intensities 18:12:7:3, as shown in Fig. 4. These numbers are in good agreement with a relativistic one-electron calculation of magnetic circular dichroism of $2p$ XPS.¹⁴⁾

§3. Continuum-Excited XES

In the previous section we calculated the XPS spectrum. These are the intermediate states of X-ray emission, and their helicity-dependent distributions determine the dichroism in the X-ray emission spectra. Excitation with circularly polarized light has produced a spin-polarized photoelectron and polarized core hole. But spin is not a good quantum number for the core hole. The spin-orbit coupling is much larger than the life-time broadening, and its spin precesses rapidly. It will not remain aligned with the spin of the photoelectron.

Let us study the $2p_{1/2}$ level first, with the help of Fig. 5. The majority (\downarrow) spin weights of the $j_m = 1/2$ and $j_m = -1/2$ core-hole states have a ratio of 1:2. If the transition rate from a completely polarized d^5 shell to the $2p_{1/2}$ $m_j = -1/2$ level is A , the transition rate to the $2p_{1/2}$ $m_j = 1/2$ level will be twice as large: $2A$. Here we assumed that the spin-orbit splitting of the $3d$ states is negligible, so that spin is a good quantum number for the valence orbitals.

Now circularly polarized light does not produce only $j_m = 1/2$ or only $j_m = -1/2$ states. Figure 4 shows that the areas of the ($j = 1/2$, $m_j = \pm 1/2$) states have a ratio of 1:3 for circularly polarized light. That means that for positive helicity 1/4 of the core hole state has $j_m = -1/2$ with a decay rate of A and 3/4 has $j_m = +1/2$ with a decay rate of $2A$, which gives an average decay rate $7/4 A$. For the negative helicity we find an average decay rate of $5/4 A$. This ratio of 7:5 is in less glaring disagreement with experiments than the ratio of 3:1 found by Jo and Parlebas.

One can also find this ratio in the $2p_{1/2}$ part of Fig. 6. There the XPS intensities from Fig. 4 have been split up according to their spin weights. One sees that the ratios are 7:5 with majority spins dominating for light with positive helicity. For arbitrary $3d$ spin occupation numbers n_\downarrow and n_\uparrow we can express the L_β MCD as $7n_\downarrow + 5n_\uparrow : 5n_\downarrow + 7n_\uparrow$. With $n_\downarrow = 5$, we find ratios of 7:5, 5:4, 45:39, 25:23, and 55:53 for $n_\uparrow = 0, 1, 2, 3$ and 4, respectively.

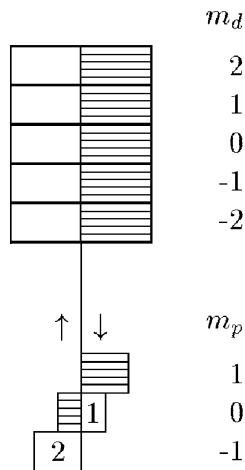


Fig. 5. A $2p_{1/2}$ core-ionized $3d^5$ atom with the hole in the $m_j = -1/2$ state. (Hatched boxes indicate occupied orbitals.) The $m_j = 1/2$ state decays twice as fast because of the larger spin overlap with occupied $3d \downarrow$ -orbitals.

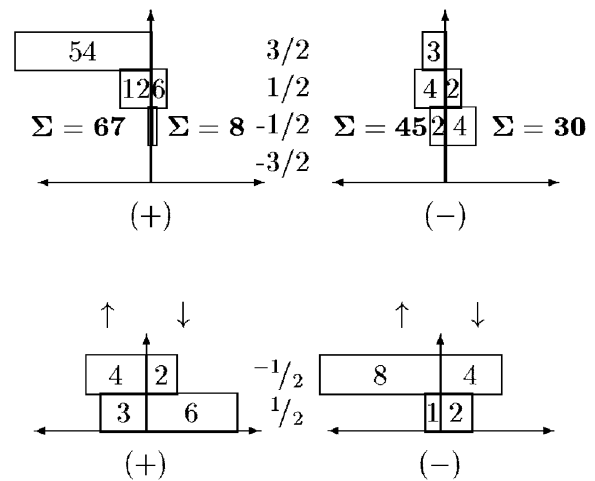


Fig. 7. Spin-weight distribution of $2p$ core levels excited on the resonances by light with positive and negative helicity.

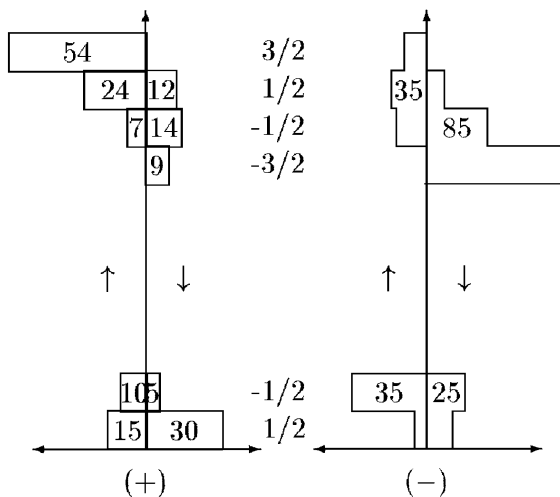


Fig. 6. Spin-weight distribution of $2p$ core levels excited to the continuum by light with positive (Left) and negative helicity (Right).

Let us now assume that the final state is screened by charge transfer, which obviously has to be a minority electron. So for ions with only minority holes, screening reduces the spin-imbalance. This effect is shown by the hatched area in Fig. 8, limited by the calculated values for unscreened and well-screened ($n + 1$) intermediate states. For Mn^{2+} , one then expects at most a dichroism of 5:4 or 25%. While still larger than experiment, this is a great improvement compared to the ratio of 2:1 predicted by Jo and Parlebas.¹¹⁾

We can take the same procedure for excitation to the L_3 -continuum. Excitation by light with positive helicity produces $2p_{3/2}$ sublevels $m_j = 3/2, \dots, -3/2$ in the ratio 18:12:7:3. The weights of the decay rates for majority (\downarrow) $3d$ spins are 0:1:2:3. The dichroism is obtained by reversing either the populations of the sublevels due to a reversal of the polarisation, or by reversing their decay rates due to a reversal of the spin direction. For majority spins this leads to a dichroism ratio of $(12 \times 1 + 7 \times 2 + 3 \times 3) : (18 \times 3 + 12 \times 2 + 7) = 35:85 = 7:17$.

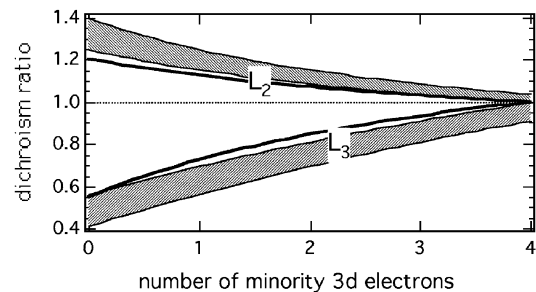


Fig. 8. Calculated dichroism ratios for resonant excitation (lines) and continuum excitation with varying amounts of screening (hatched areas).

This gives stronger dichroism than predicted by Jo and Parlebas,¹¹⁾ which already was larger than experiment. The resolution of this discrepancy may lie in the fact that our calculated XPS spectrum is not correct. Our single-particle picture gave equal intensities to the four m_j levels for unpolarized light, but this is not correct. For example, the $2p_{3/2}$ peak of MnF_2 clearly shows multiplet structure with ratios of approximately 9:7:5:3, multiplicities given by the total $2j + 1$ of the Mn final state.¹⁵⁾

§4. Resonance-Excited XES

For excitation on resonance, a single-particle model is even less appropriate than for continuum excitation, but it is straightforward to do the exercise. In contrast to Jo and Parlebas, we assume that the fluorescence signal is saturated and that positive and negative helicity light create equal numbers of holes. This is a good approximation for experiments on concentrated bulk samples with grazing incidence and near-normal detection. We start at the L_2 edge. The decay rate of an $m_j = 1/2$ hole is $(n_{\uparrow} + 2n_{\downarrow})A$ and the decay rate of an $m_j = -1/2$ hole is $(2n_{\uparrow} + n_{\downarrow})A$. With positive-helicity light the ratio of states with $j_m = 1/2$ to states with $j_m = -1/2$ is 3:2 (the areas on the spin-up side of Fig. 3). We find for positive helicity an average decay rate of

$(3(n_{\uparrow}+2n_{\downarrow})+2(2n_{\uparrow}+n_{\downarrow}))/5 A = (7n_{\uparrow}+8n_{\downarrow})/5 A$. With negative-helicity light the ratio of states with $j_m = 1/2$ to states with $j_m = -1/2$ is 1:4. We find for negative helicity an average decay rate of $(n_{\uparrow}+2n_{\downarrow}+4(2n_{\uparrow}+n_{\downarrow}))/5 A = (9n_{\uparrow}+6n_{\downarrow})/5 A$. One must take into account the excited electron. Assuming that its orbital moment is quenched, we can express the L_2 MCD on resonance as $7(n_{\uparrow}+1)+8n_{\downarrow}:9(n_{\uparrow}+1)+6n_{\downarrow}$. With $n_{\downarrow} = 5$, we find ratios of 47:39, 54:48, 61:57, 68:66, and 1:1. Taking into account the m_j levels results in numbers on resonance that are different from the MCD ratio off resonance with a screening electron added.

Finally the L_3 MCD on resonance. The core hole states with $m_j = 3/2, \dots, -3/2$ are created in ratios of 18:6:1:0 for positive light and of 1:2:2:0 for negative light. These ratios are used in drawing Fig. 7, from which we find the dichroism ratio $67(n_{\uparrow}+1)+8n_{\downarrow} : 45(n_{\uparrow}+1)+30n_{\downarrow}$. With $n_{\downarrow} = 5$, we find ratios of 107:195, 174:240, 241:285, 308:330, and 1:1.

§5. Conclusion

Figure 8 summarizes my results. The lines give the calculated dichroism in the so-called ‘‘thick limit’’, where the total number of core holes within view of the detector is saturated, and does not depend on the absorption cross section and its dichroism. That is why the curves decay to unity with decreasing spin-polarisation in the $3d$ shell. Both at the L_3 and at the L_2 edges, the absorption dichroism is opposite to the emission dichroism. This is in agreement with experiment for continuum excitation. For resonant excitation, the experimental situation is more complex, because one needs to separate the effects of the absorption dichroism and of dichroic elastic scattering. Duda⁴⁾ shows how the measured emis-

sion dichroism of cobalt depends on the sample thickness and on the angle of incidence. The observed reversal of sign at the L_3 edge shows that also here the emission dichroism is opposite to and weaker than the absorption dichroism.

Acknowledgement

The author thanks Akademikernas Erkända A-kassa for financial support.

-
- 1) C. T. Chen, F. Sette, Y. Ma and S. Modesti: Phys. Rev. **42** (1990) 7262.
 - 2) L. Baumgarten, C. M. Schneider, H. Petersen, F. Schäfers and J. Kirschner: Phys. Rev. Lett. **65** (1990) 492.
 - 3) P. Strange, P. J. Durham and B. L. Georffy: Phys. Rev. Lett. **67** (1991) 3590.
 - 4) L.-C. Duda, J. Stöhr, D. C. Mancini, A. Nilsson, N. Wassdahl, J. Nordgren and M. G. Samant: Phys. Rev. B **50** (1994) 16758; L.-C. Duda: thesis Uppsala University (unpublished).
 - 5) C. F. Hague, J.-M. Mariot, P. Strange, P. J. Durham and B. L. Georffy: Phys. Rev. B **48** (1993) 3560.
 - 6) S. Eisebitt, J. Lüning, J.-E. Rubensson, D. Schmitz, S. Blügel and W. Eberhardt: Solid State Commun. **104** (1997) 173.
 - 7) L. Braicovich, C. Dallera, G. Ghiringhelli, N. B. Brookes and J. B. Goedkoop: Phys. Rev. B **55** (1997) 14729.
 - 8) G. van der Laan and B. T. Thole: Phys. Rev. B **43** (1991) 3306.
 - 9) J. L. Erskine and E. A. Stern: Phys. Rev. B **12** (1975) 5016.
 - 10) T. Jo: Synchrotron Radiation News **5** No. 2 (1992) 21.
 - 11) T. Jo and J.-C. Parlebas: J. Phys. Soc. Jpn. **68** (1999) 1392.
 - 12) T. Jo: J. Electron Spectr. Rel. Phen. **86** (1997) 73.
 - 13) Several Web-sites offer $3j$ -symbol calculators, e.g. <http://plasma-gate.weizmann.ac.il/369j.html>.
 - 14) H. Ebert, L. Baumgarten, C. M. Schneider and J. Kirschner: Phys. Rev. B **44** (1991) 4406.
 - 15) S. P. Kowalczyk, L. Ley, F. R. McFeely and D. A. Shirley: Phys. Rev. B **11** (1975) 1721.